Rapid Cycling of Lipid Raft Markers between the Cell Surface and Golgi Complex[✪]

Benjamin J. Nichols,* Anne K. Kenworthy,* Roman S. Polishchuk,* Robert Lodge,* Theresa H. Roberts,* Koret Hirschberg,* Robert D. Phair,[‡] and Jennifer Lippincott-Schwartz*

*Cell Biology and Metabolism Branch, National Institute of Child Health and Human Development, Bethesda, Maryland 20895; and [‡]BioInformatics Services, Rockville, Maryland 20854

Abstract. The endocytic itineraries of lipid raft markers, such as glycosyl phosphatidylinositol (GPI)-anchored proteins and glycosphingolipids, are incompletely understood. Here we show that different GPI-anchored proteins have different intracellular distributions; some (such as the folate receptor) accumulate in transferrin-containing compartments, others (such as CD59 and GPI-linked green fluorescent protein [GFP]) accumulate in the Golgi apparatus. Selective photobleaching shows that the Golgi pool of both GPI-GFP and CD59-GFP constantly and rapidly exchanges with the pool of these proteins found on the plasma membrane (PM). We visualized intermediates carrying GPI-GFP from the Golgi apparatus to the PM and separate structures delivering GPI-GFP to the Golgi apparatus.

GPI-GFP does not accumulate within endocytic compartments containing transferrin, although it is detected in intracellular structures which are endosomes by the criteria of accessibility to a fluid phase marker and to cholera and shiga toxin B subunits (CTxB and STxB, which are also found in rafts). GPI-GFP and a proportion of the total CTxB and STxB taken up into cells are endocytosed independently of clathrin-associated machinery and are delivered to the Golgi complex via indistinguishable mechanisms. Hence, they enter the Golgi complex in the same intermediates, get there independently of both clathrin and rab5 function, and are excluded from it at 20°C and under conditions of cholesterol sequestration. The PM–Golgi cycling pathway followed by GPI-GFP could serve to regulate lipid raft distribution and function within cells.

Key words: Golgi complex • endocytes • glycosyl phosphatidylinositol anchor • raft • green fluorescent protein

Introduction

A functionally diverse set of cell surface proteins, including receptors, adhesion molecules, and enzymes, become insoluble to extraction in the detergent Triton X-100 as they traverse the secretory pathway and are delivered to the plasma membrane (PM).[1] Acquisition of resistance to detergent extraction is thought to correspond to assembly into stable microdomains, which can be conceptualized as lipid rafts floating in the membrane (Simons and Ikonen, 1997; Pralle et al., 2000). Purification of detergent-resistant membranes shows that they are enriched in sterols, glycosphingolipids, sphingolipids, saturated phospholipids, and glycosyl phosphatidyl inositol (GPI)-anchored proteins (Simons and Ikonen, 1997; Brown and London, 1998). Lipid rafts, as defined by detergent resistance, have been associated with sorting of proteins bound for the cell surface during exit from the Golgi complex, as well as with organization of signaling molecules on the cell surface (Simons and Ikonen, 1997; Stauffer and Meyer, 1997; Brown and London, 1998). The lateral heterogeneity within individual cell membranes generated by rafts could thus play a crucial role in processes as diverse as signal transduction and cell polarity.

Given the range of important cell biological roles attributed to lipid rafts, a detailed understanding of the manner in which rafts are removed from and potentially recycled back to the cell surface is an important goal. To clarify the intracellular pathways followed by rafts we have investigated the transport itineraries of two main classes of raft markers, GPI-anchored proteins and the lipid-binding

[✪]The online version of this article contains supplemental material.

B. Nichol's present address is Laboratory of Molecular Biology, Medical Research Council, Cambridge CB2 2QH, UK.

Address correspondence to Jennifer Lippincott-Schwartz, Cell Biology and Metabolism Branch, National Institute of Child Health and Human Development, Building 18T, Library Drive, Bethesda, MD 20895-0001. Tel.: (301) 402-1010. Fax: (301) 402-0078. E-mail: jlippin@helix.nih.gov

[1]*Abbreviations used in this paper:* CFP, cyan fluorescent protein; CTxB, cholera toxin B; GFP, green FP; GPI, glycosyl phosphatidylinositol; NRK, normal rat kidney; PM, plasma membrane; STxB, shiga TxB; YFP, yellow FP.

subunits of specific bacterial toxins. The lipid moiety of GPI-anchored proteins is sufficient for incorporation into the detergent-resistant membranes of rafts (Benting et al., 1999). These proteins undergo endocytosis, most likely by both clathrin-dependent and -independent mechanisms, but in most cases subsequent intracellular trafficking remains little understood (Lisanti et al., 1990; Rothberg et al., 1990; Parton et al., 1994; Fransson et al., 1995; Smart et al., 1996; Skretting et al., 1999). The GPI-anchored protein that has been characterized most extensively in terms of its endocytic itinerary, the folate receptor, is taken up into transferrin-labeled endocytic compartments (Mayor et al., 1998; Varma and Mayor, 1998). However, there is at least one published example of a GPI-anchored protein (a GPI-anchored heparan sulfate proteoglycan) that appears to be delivered to the Golgi complex after internalization from the cell surface (Fransson et al., 1995), suggesting that different GPI-anchored proteins traffic differently, possibly because of sorting signals in their ectodomains (Zurzolo et al., 1993; Benting et al., 1999). In this study we used markers for a variety of GPI-anchored proteins, including folate receptor, CD59 (Davies and Lachmann, 1993), and a construct composed of GPI-anchored green fluorescent protein (GPI-GFP). Because GPI-GFP lacks identifiable sorting signals other than the GPI anchor itself, its distribution is likely to represent only the interaction of the GPI anchor with other cell surface lipid components.

The lipid-binding B subunits of shiga and cholera toxins (STxB and CTxB, respectively) are the second class of markers we used for studying the uptake of lipid rafts. These markers are found in detergent-resistant membrane fractions (Orlandi and Fishman, 1998; Katagiri et al., 1999). CTxB and STxB bind to the glycosphingolipids GM1 and Gb3, respectively, at the cell surface. As is the case with GPI-anchored proteins, previous work has revealed that the endocytic itineraries of these toxins are complex. Studies on internalization of CTxB have generally focussed on a clathrin-independent mechanism, whereas STxB is thought to enter the cell via clathrin-coated pits (Sandvig et al., 1989; Orlandi and Fishman, 1998). After internalization both toxin subunits are delivered to the Golgi complex, from which STxB subsequently is slowly delivered to the ER (Mallard et al., 1998).

Using time-lapse fluorescence microscopy and selective photobleaching techniques, we have followed the intracellular itineraries of lipid raft markers. We found that, unlike the folate receptor, CD59 and GPI-GFP do not accumulate within transferrin-labeled endosomes (Mayor et al., 1998). Instead, these raft markers continuously cycle between the PM and the Golgi complex. GPI-GFP is excluded from clathrin-coated pits and reaches the Golgi apparatus independently of both clathrin-interacting endocytic machinery and rab5. CTxB and STxB follow the same pathway as GPI-GFP and CD59 from the cell surface to the Golgi complex, but they also accumulate in transferrin-labeled endosomes. Reduced cholesterol levels or incubation at 20°C inhibit trafficking of GPI-GFP and delivery of CTxB and STxB to the Golgi complex, without preventing uptake into transferrin-containing endosomes.

Materials and Methods

DNA Constructs and Cell Transfection

Transient transfections were carried out using FuGENE™ 6 (Roche). Stable cell lines were produced by selection for G418 resistance. The GPI-GFP construct was from S. Lacey (Southwestern University, TX), GPI-yellow fluorescent protein (YFP) was from M. Edidin (Johns Hopkins University, Baltimore, MD) Plasmids expressing VSV-Gts045-CFP and GalT-CFP were derived, by exchange of GFP for cyan fluorescent protein (CFP), from constructs described previously (Presley et al., 1997; Zaal et al., 1999). The CD59-GFP–expressing plasmid was produced by inserting CD59 cDNA between the EcoRI and BglII sites of plasmid ss-GFP (Nehls et al., 2000). Rab5S34N and Q79L were created by PCR site–directed mutagenesis and cloned KpnI/BamHI into pEGFPc1 and appropriate spectral variants (CLONTECH Laboratories, Inc.). The plasmid expressing dominant negative epsin mutant (just the DPW domain of epsin) was from P. DeCamilli (Yale University, New Haven, CT; Chen et al., 1998). Plasmid-expressing Eps15 mutant (D95/295) was from A. Benmerah (Institut Pasteur, Paris, France; Benmerah et al., 1999)

Labeling with Antibody and Fluorescent Ligands

The following antibodies were used: monoclonal anti-mannosidaseii (Zaal et al., 1999), monoclonal anti-CD59 and monoclonal antifolate receptor (Kenworthy and Edidin, 1998), polyclonal anti-GFP (Molecular Probes), and monoclonal anti-FLAG epitope (Sigma-Aldrich). Secondary antibodies were from Southern Biotechnology Associates, Inc. 10K dextran conjugated to Fluoro-Ruby™ was from Molecular Probes. Immunofluoresence protocol was as described (Zaal et al., 1999). CTxB and human holotransferrin were from Sigma-Aldrich. Cross-linkable Cy5 or Cy3 fluorophores were conjugated to CTxB or transferrin according to the manufacturer's instructions (Amersham Pharmacia Biotech). STxB subunit was from L. Johannes (Institut Curie, Paris, France). For labeling COS-7 or HeLa cells, transferrin was used at 5 μg/ml; for normal rat kidney (NRK) cells, 25 μg/ml was used. CTxB and STxB were used at 1 μg/ml. Cells were fixed or imaged after 25 min uptake unless otherwise indicated.

Antibody uptake experiments consisted of precooling cells on ice, adding Cy3-transferrin (5 μg/ml) and 9E10 anti-myc antibody (0.1 μg/ml) for 10 min, washing into prewarmed DME, and allowing uptake for the times indicated before fixation distribution of 9E10 after uptake was ascertained with a Cy5-conjugated secondary antibody.

Triton X-100, Cycloheximide, and Filipin Treatment

In Triton X-100 extraction experiments, live cells were cooled to 4°C, washed into ice cold 1% Triton X-100 in PBS, left for 20 min, then washed into 2% formaldehyde in PBS, and fixed as usual. Cycloheximide was used at 200 μg/ml for COS-7 cells and 25 μg/ml for other cell lines. Filipin was used at the concentrations indicated, all images shown are of cells treated for 45 min and then fixed. Filipin and cycloheximide were from Sigma-Aldrich.

Microscopy

All fluorescence images were obtained using a confocal microscope (LSM510; ZEISS). Excitation wavelengths and filter-sets for GFP, YFP, CFP, Cy3, rhodamine, and Cy5 were as supplied by the manufacturer or described previously (Zaal et al., 1999). Images of fixed cells not intended for quantification of fluorescence intensities were taken using 63× 1.4 NA or 100× 1.4 NA objectives with the confocal pinhole set to one Airey unit. Live cell images and images intended for quantitative analysis were obtained with a 40× 1.3 NA objective and the confocal pinhole set fully open. Selective photobleaching was carried out on the ZEISS LSM510 using 75 consecutive scans with a 488-nm laser line at full power. Live cells were held at 35°C.

To stain GPI-GFP for immunoelectron microscopy, transfected cells were fixed and incubated with anti-GFP antibody (Molecular Probes) as described (Polishchuk et al., 2000). Then the cells were labeled with Nanogold-conjugated secondary antibody and Gold Enhance kit (Nanoprobes, Inc.) and processed for embedding and cutting according routine protocols.

Image Analysis

For 8-bit color images, pixel intensity levels were adjusted using Adobe Photoshop® so that maximal and minimal values were ~0 and 255 in each channel.

For quantitation of overlap between different markers, images were thresholded by eye to produce a binary representation of structures where a given marker was enriched. Such images for both markers to be compared were combined using a logical *and*, so as to yield an image of only those pixels which were positive in both of the binary images. Then the total number of pixels in each of the binary images and the combined image were compared to give a percentage of those pixels containing one marker that also contained the other. The Golgi region was excluded from the analysis. Values given represent the mean from three separate cells.

In Quicktime movies the contrast of original images was in some cases increased. Quicktime movies employ the Cinepak compression algorithm and were produced using Adobe Premiere®. Quantitation of mean fluorescence intensity in selected regions of interest was carried out using NIH Image. All measurements of fluorescence intensity were background-corrected, and where necessary corrected for partial photobleaching during image collection.

Kinetic Analysis

Standard methods of compartmental analysis were used (Jacquez, 1996; Hirschberg et al., 1998). A model of GPI-GFP trafficking was developed that includes ER processing, transport to the Golgi complex, exchange with the large PM pool, and, ultimately, protein turnover. A special feature of the GPI analysis is a compartment representing the fraction of the PM pool that is visualized over the Golgi region. Data in the Golgi region of interest were fitted to the sum of the Golgi compartment and the compartment representing overlaying PM. All the rate constants could then be estimated with coefficients of variation between 8 and 13%, using the optimizer included in the SAAM II (SAAM Institute) software.

Online Supplemental Material

Quicktime movies alluded to in Results are available at http://www.jcb.org/cgi/content/full/153/3/529/DC1. Video 1 shows recovery of the Golgi pool of GPI-GFP after photobleaching (Fig. 2). Video 2 shows depletion of the Golgi pool of GPI-GFP as a consequence of depletion of the PM pool by repetitive photobleaching (Fig. 2). Video 3 shows exocytic transport intermediates carrying GPI-GFP out from the Golgi (Fig. 3). Video 4 shows endocytic transport intermediates delivering STxB, CTxB, and GPI-GFP to the Golgi complex (Fig. 5).

Results

Steady-State Localization of GPI-GFP and CD59 in PM and Golgi Membranes

GPI-GFP behaved as a lipid raft–associated protein, being incorporated into detergent-resistant domains. When cells were extracted with 1% Triton X-100 before fixation, GPI-GFP was resistant to this treatment, whereas vesicular stomatitis virus G protein was efficiently removed (Fig. 1 A; Mayor and Maxfield, 1995). The steady-state distribution of GPI-GFP in COS-7, NRK, HeLa, and MDCK cells included two major pools, one at the cell surface and one in a juxtanuclear compartment (Fig. 1 B). This compartment (see boxed area in Fig. 1 B) was identified as the Golgi complex rather than recycling endosomes (which frequently have a similar distribution) by colocalization with a Golgi resident enzyme, mannosidase II, and lack of colocalization with endocytosed transferrin (Fig. 1, C and D). Typically, 90% of the total cellular GPI-GFP fluorescence appeared on the cell surface, whereas ~10% was found in the Golgi complex.

We next asked whether there are endogenous GPI-anchored proteins that share the same distribution as GPI-GFP. Antibody staining of HeLa cells expressing GPI-GFP showed that CD59, a ubiquitous GPI-anchored protein (Davies and Lachmann, 1993), is also found both in a juxtanuclear, intracellular pool and on the cell surface, even after prolonged cycloheximide treatment to chase nascent protein out of the secretory pathway (Fig. 1 E). The juxtanuclear pool colocalized extensively with GPI-GFP and was further identified as the Golgi complex by labeling with antibodies against the Golgi protein GM130. A chimera with GFP fused to the NH_2 terminus of CD59 (CD59-GFP) expressed in NRK cells also had a distribution similar to that of GPI-GFP and endogenous CD59. This included a juxtanuclear pool that colocalized with mannosidase II after cycloheximide treatment, but not with transferrin-containing recycling endosomes (Fig. 1 F, data not shown). In contrast, antibodies against another GPI-anchored protein, the folate receptor, stained structures which were separate from the Golgi complex, many of which could be labeled with endocytosed transferrin (Fig. 1 G; Mayor et al., 1998). These observations indicate that GPI-GFP, CD59, and a GFP fusion based on CD59 are found in both the PM and the Golgi complex, whereas a third GPI-anchored protein, the folate receptor, has a different distribution that overlaps with transferrin-containing endosomes.

Constitutive Cycling of GPI-GFP between the Golgi Complex and Cell Surface

As a direct test of whether the Golgi pool of GPI-GFP is dependent on a flux of newly synthesized protein from the ER, GPI-GFP–expressing cells were incubated in cycloheximide (which blocks protein synthesis) for 5 h, and the ratio between the mean fluorescence intensity of the Golgi region and that of the rest of the cell was calculated at different time points (Fig. 2 C). The relative Golgi fluorescence of GPI-GFP declined slightly during the first 2 h of the experiment, but then remained constant. This suggests that only a small proportion (15–25%) of Golgi fluorescence is derived from newly synthesized GPI-GFP, with the remainder the result of active maintenance of GPI-GFP in the Golgi complex.

Selective photobleaching provided a direct way of addressing whether GPI-GFP in the Golgi complex exchanges with GPI-GFP on the PM. The Golgi pool of GPI-GFP was selectively photobleached in cells where protein synthesis had been inhibited, and recovery of fluorescence into the Golgi region was followed over time (Fig. 2 A and Video 1). After bleaching the Golgi region, there was no increase in total cellular fluorescence (since protein synthesis was inhibited). Nevertheless, Golgi fluorescence rapidly recovered as cell surface fluorescence decreased. The ratio between mean fluorescence intensity in the Golgi region and that outside of this region returned to the same value as was observed before the bleach, implying that all of the GPI-GFP in the Golgi region is constantly exchanging with the non-Golgi pool (i.e., the PM). Photobleaching of the Golgi pool of CD59-GFP under the same conditions gave similar results (Fig. 2 B), and, as described above, the Golgi pool of endogenous CD59 was not chased out by addition of cycloheximide. This implies that the Golgi pools of endogenous CD59, CD59-GFP,

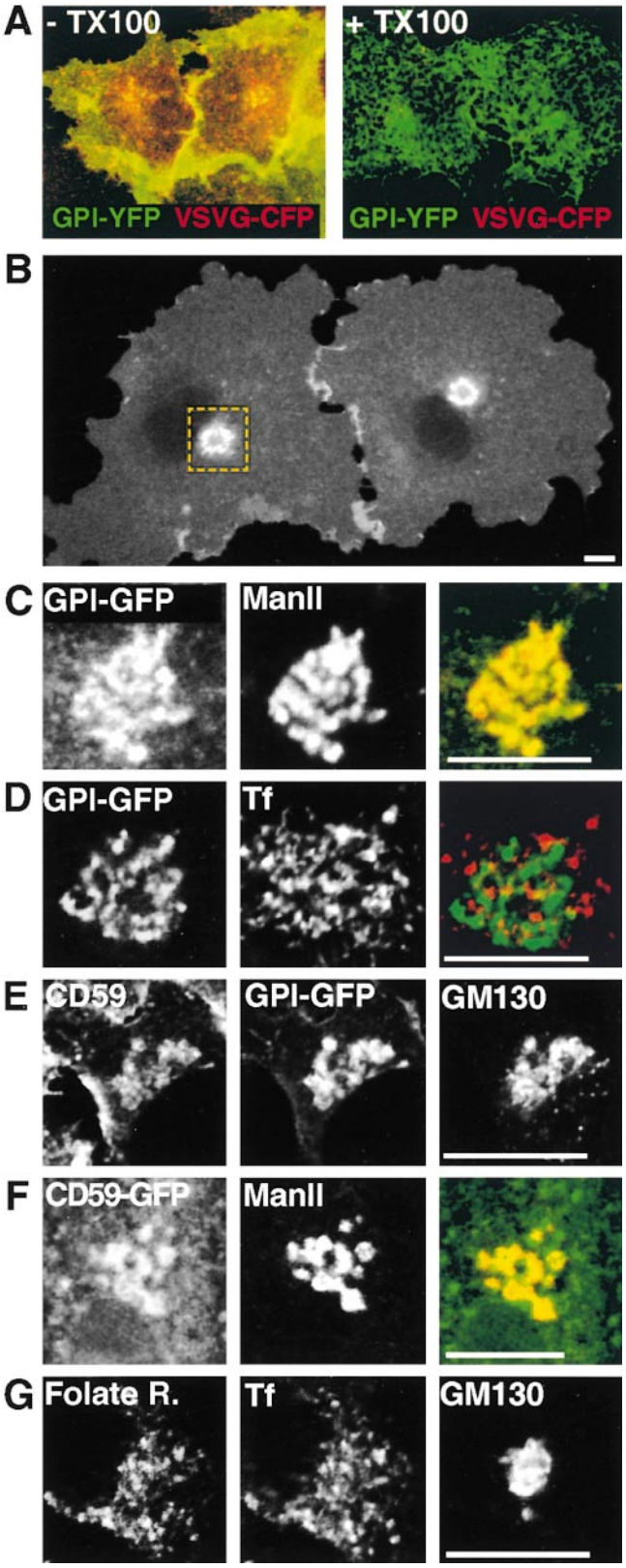

Figure 1. Localization of specific GPI-anchored proteins to the Golgi complex. (A) Triton X-100 extraction of COS-7 cells expressing GPI-CFP (green) and VSVG-YFP (red). (B) GFP fluorescence from GPI-GFP expressed in COS-7 cells. Similar distributions were seen in NRK, HeLa, and MDCK cells. (C) Immunofluorescence staining comparing the distribution of a Golgi enzyme, mannosidase II, with that of the perinuclear pool of GPI-GFP in NRK cells. Only a restricted region of the cell, equivalent to the boxed area in A, is shown. (D) Perinuclear distribution of Cy3-transferrin and GPI-GFP in NRK cells. (E) Triple-labeling of a HeLa cell for endogenous CD59, GPI-GFP, and the Golgi marker GM130. (F) Comparison of CD59-GFP and mannosidase II distributions in COS-7 cells. (G) Triple-labeling of a HeLa cell for endogenous folate receptor, Cy3-transferrin, and GM130. Bars, 5 mm.

and GPI-GFP are maintained by constant exchange with the PM, rather than by new protein synthesis.

Kinetic analysis of quantitative data obtained from the photobleaching experiments permitted an estimation of the rate constants characterizing transport of GPI-GFP between PM and Golgi complex (Fig. 2 D). Standard methods of kinetic analysis were used, with the PM and Golgi pools of GPI-GFP treated as two compartments exchanging via first order processes, each with a characteristic rate constant (see Materials and Methods). Least squares fitting of these data yielded 0.111 min^{-1} as the rate constant governing GPI-GFP transport from Golgi to PM, and 0.0042 min^{-1} for PM to Golgi transport. Given these rate constants, an average GPI-GFP molecule resides in the PM for ~200 min and in the Golgi complex for ~9 min (mean residence time in a given compartment being the reciprocal of the rate constant for exit from that compartment).

Repetitive photobleaching of a small area of the PM eliminated GPI-GFP fluorescence from the entire PM pool and gradually depleted the Golgi pool to 10–20% of its initial fluorescence intensity (Fig. 2 E and Video 2), as expected if GPI-GFP fluorescence in the Golgi complex is dependent on constant supply from the PM. The cells in this experiment were not treated with cycloheximide, so the data again imply that the majority of the steady-state pool of GPI-GFP in the Golgi complex is dependent on constant exchange with the PM.

We used an independent approach to confirm that GPI-GFP returns to the Golgi after exposure at the cell surface. GPI-GFP with an additional *myc* epitope was expressed in COS-7 cells. Anti-*myc* antibody was taken up to the Golgi apparatus in transfected cells, whereas no internalization of antibody was detected in neighboring nontransfected cells (Fig. 2 F).

Exocytic Transport Intermediates Containing GPI-GFP

Continuous cycling of GPI-GFP between the Golgi and the cell surface implies that GPI-GFP should be present in both exocytic and endocytic transport intermediates. To resolve exocytic intermediates carrying GPI-GFP out from the Golgi, the non-Golgi pool of GPI-GFP was eliminated by photobleach. Subsequent time-lapse imaging revealed numerous transport intermediates containing GPI-GFP rapidly emerging from the Golgi complex (Fig. 3 and Video 3, A and B). These transport intermediates appeared as small spherical or tubular structures and they moved along curvilinear tracks (Video 3, A and B). No motile transport intermediates were seen when microtubules were depolymerized with nocodazole treatment (data not shown). Intermediates were still observed in cycloheximide-treated cells. The PM fluorescence gradually recovered after the

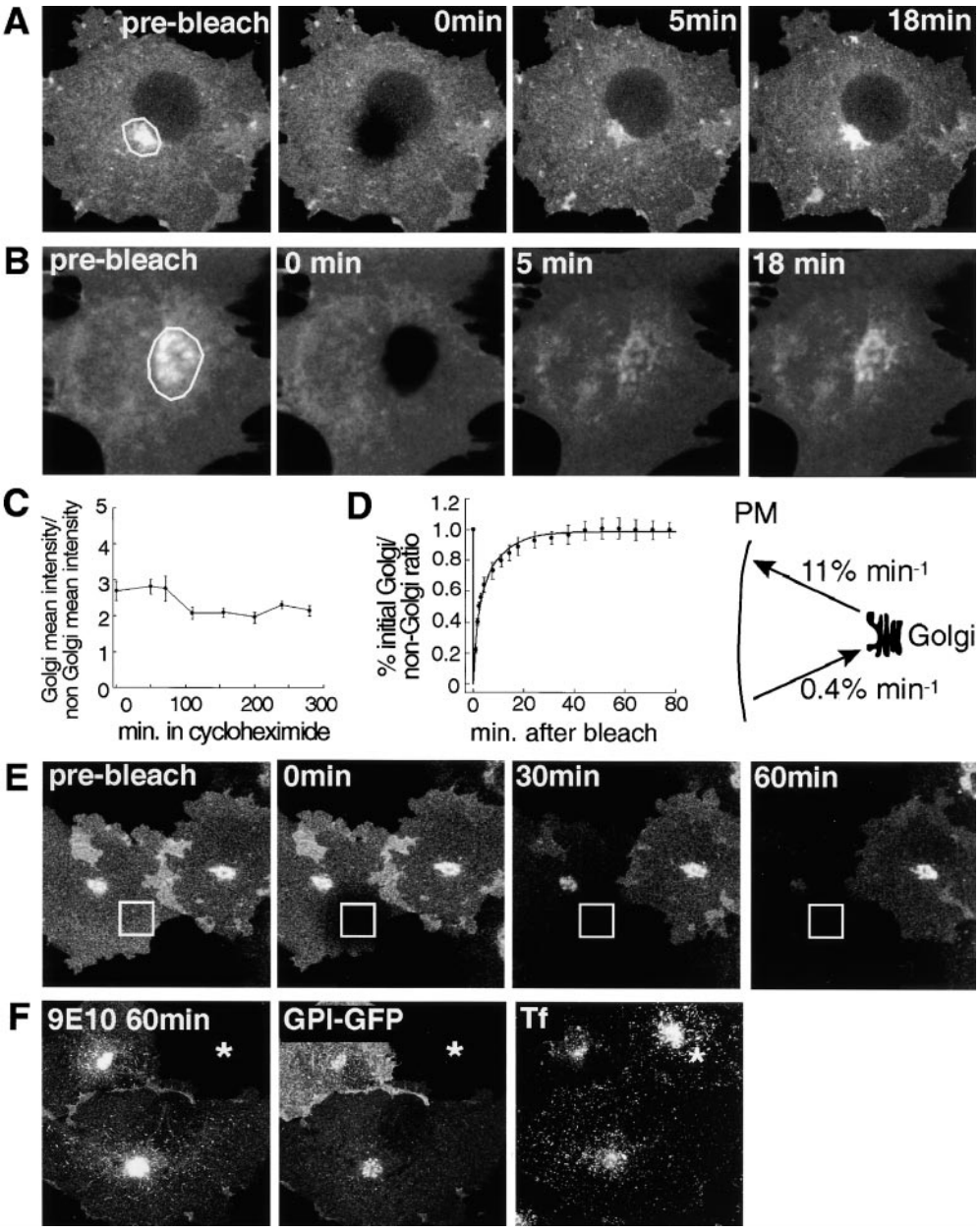

Figure 2. Constitutive cycling of GPI-GFP and CD59-GFP between the Golgi complex and the PM. (A) The Golgi pool of GPI-GFP recovers rapidly after photobleach. The area enclosed by a white line in the prebleach image was photobleached. The times shown in the second two panels denote minutes postbleach. COS-7 cells were pretreated with 200 μg/ml cycloheximide for 2 h before photobleaching. (B) The Golgi pool of CD59-GFP recovers rapidly after photobleach. The experiment was carried out as in Fig. 1 C. (C) The Golgi pool of GPI-GFP is not dependent on new protein synthesis. The ratio between mean fluorescence intensity in the Golgi region and mean fluorescence intensity in the rest of the cell is then plotted as a function of time after addition of 200 μg/ml cycloheximide to COS-7 cells. $n \geq 15 \pm$ SE. (D) The Golgi pool of GPI-GFP recovers after photobleach; quantitation and kinetics. The Golgi pool of GPI-GFP was eliminated by photobleach as shown in C. Mean fluorescence intensity of Golgi and non-Golgi pools was determined at the times indicated and expressed as a percentage of the prebleach ratio between these values (filled circles). These data were applied to a kinetic model (see Materials and Methods) so as to derive rate constants describing exchange between Golgi and PM pools. The solid line gives the recovery curve predicted by this model, and rate constants are shown in the adjacent cartoon. Cells were pretreated with 200 μg/ml cycloheximide for 2 h before the experiment. $n = 6 \pm$ SE. (E) Depletion of the cell surface pool of GPI-GFP by repeated photobleaching leads to depletion of the Golgi pool. The area enclosed by a white box was completely photobleached every minute. Cells were not cycloheximide treated. (F) Anti-myc antibody 9E10 is endocytosed to the Golgi complex specifically in cells expressing (myc-tagged) GPI-GFP. Antibody uptake experiments are described in detail in Materials and Methods. The asterisk highlights a cell not expressing GPI-GFP, but labeled with Cy3-transferrin. The perinuclear clustering of transferrin in cells after 60 min of uptake represents recycling endosomes which are devoid of GPI-GFP (Fig. 1 D). Supplemental video available at http://www.jcb.org/cgi/content/full/153/3/529/DC1.

photobleach (Fig. 3), so the intermediates appear to function in delivery of GPI-GFP to the cell surface.

GPI-GFP Is Found in Endocytic Structures That Contain STxB and CTxB, but Not Transferrin

We examined narrow optical sections of fixed cells that had been labeled with several endocytic markers. A high proportion of those GPI-GFP–positive structures found scattered throughout the cytoplasm were labeled with 10K dextran after a 15 min uptake (36% of pixels in GPI-GFP–positive structures were also positive for dextran; see Materials and Methods; Fig. 4 A). Those GPI-GFP structures that did not contain dextran could well represent separate exocytic intermediates, as visualized in Fig. 3. GPI-GFP–positive structures did not overlap with endocytosed transferrin after continuous uptake for 20 min (2.5% of pixels in GPI-GFP structures contained transferrin; Fig. 4 B) or after shorter periods of uptake (data not shown). Furthermore, GPI-GFP–containing structures did not colocalize

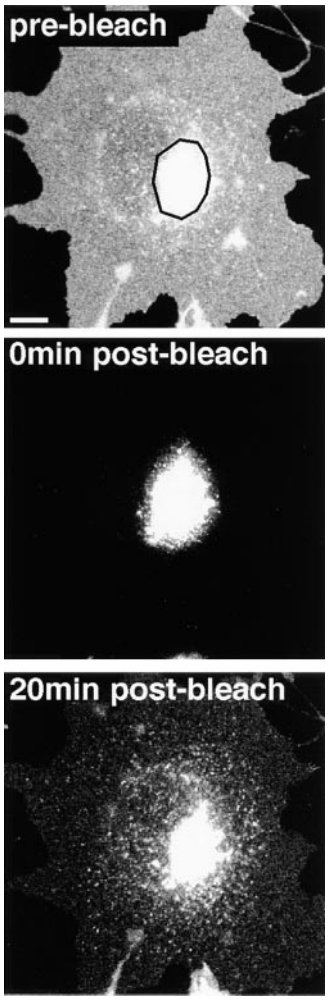

Figure 3. Exocytic transport intermediates carrying GPI-GFP. GPI-GFP was expressed in COS-7 cells. All fluorescence outside of the region indicated in the pre-bleach image was eliminated by photobleaching. Note that the fluorescence intensity of the Golgi region is saturated (pixel value equals 255 for 8-bit images) in all of these images to allow visualization of the less bright transport intermediates. Times in subsequent panels are relative to the end of the photobleach. Supplemental video available at http://www.jcb.org/cgi/content/full/153/3/529/DC1. Bar, 5 μm.

with the early endosomal marker EEA1 (3% of pixels in GPI-GFP structures contained EEA1; Fig. 4 C; Stenmark et al., 1996).

We next ascertained the distribution of STxB and CTxB, which, like GPI-GFP, are associated with lipid rafts and traffic from the cell surface to the Golgi complex. The intracellular distribution of structures containing CTxB after 30 min of continuous uptake from the PM was very similar to that of STxB, although PM labeling was stronger for CTxB (87% of pixels in CTxB structures contained STxB; Fig. 4 D), arguing that STxB and CTxB share common endocytic trafficking pathways. In GPI-GFP–expressing cells, many of the endocytic structures containing CTxB or STxB also contained GPI-GFP (42% of pixels in CTxB structures contained GPI-GFP, 71% of pixels in GPI-GFP structures contained CTxB; Fig. 4 E, not shown in the case of STxB). Those that did not contain GPI-GFP are likely to represent transferrin-containing endosomes, since endocytosed STxB and CTxB also partially colocalized with transferrin-labeled early and recycling endosomes (30% of pixels in CTxB structures contained Tf; Fig. 4 F). The presence of STxB in these endosomal compartments has been reported previously (Mallard et al., 1998). Thus, GPI-GFP accumulates to detectable levels in a population of endocytic structures which contain STxB and CTxB, but not transferrin receptor or EEA1, whereas STxB and CTxB are found both in GPI-GFP–labeled endocytic structures and those which contain transferrin.

GPI-GFP, CTxB, and STxB Enter the Golgi Complex in the Same Transport Intermediates

We used selective photobleaching and time-lapse imaging to visualize delivery of GPI-GFP to the Golgi complex. A series of images of a small region of the cell adjacent to the Golgi complex were rapidly collected immediately after photobleaching of the GPI-GFP fluorescence associated with the Golgi complex and the surrounding area (Video 4, A–D). Small transport intermediates containing GPI-GFP were observed tracking into the photobleached Golgi region where they disappeared, presumably due to fusion with the Golgi complex and subsequent dispersal of fluorescence. GPI-GFP–expressing cells were labeled with STxB and CTxB and the same photobleaching protocol was followed. As shown in Fig. 5, A and B, both STxB and CTxB were seen in GFP-GPI–containing structures that moved in towards the Golgi complex. We also detected additional intermediates containing STxB or CTxB but not GPI-GFP (not shown in Fig. 5; see Video 4, A–D), which could represent CTxB and STxB within transferrin-containing endosomes localized near the Golgi complex. Our results indicate that the transport itinerary of GPI-GFP to the Golgi complex overlaps with that of STxB and CTxB.

GPI-GFP and a Proportion of STxB and CTxB Are Internalized via a Clathrin-independent Process

To investigate whether uptake and consequent delivery to the Golgi complex of GPI-GFP, STxB, and CTxB requires clathrin-dependent endocytic machinery, we used dominant negative mutants of epsin and eps15, proteins necessary for clathrin-mediated endocytosis (Chen et al., 1998; Benmerah et al., 1999). In cells transiently transfected or microinjected with a plasmid expressing epsin or eps15 mutants, transferrin uptake was reduced significantly more than uptake of CTxB and STxB (Fig. 6, A and B; quantitation in Fig. 6 D). This differential effect is consistent with only a proportion of the total CTxB and STxB being internalized via the same endocytic machinery as transferrin, implying that the remainder may use a clathrin-independent mechanism. Importantly, CTxB and STxB were still efficiently delivered from the PM to the Golgi complex in the absence of clathrin-mediated internalization (Fig. 6 C).

We examined the rate of GPI-GFP cycling between the Golgi and the PM by using photobleaching techniques in cells expressing mutants of epsin. Cells were microinjected with the epsin mutant plasmid, left for 6 h to allow expression, and then the Golgi pool of GPI-GFP fluorescence was photobleached. Recovery of Golgi fluorescence in the mutant cells was no different than in noninjected cells (Fig. 6 E). Thus, whereas transferrin uptake requires epsin, eps15, and the clathrin-dependent endocytic machinery, delivery of GPI-GFP, STxB, and CTxB from PM to Golgi complex does not.

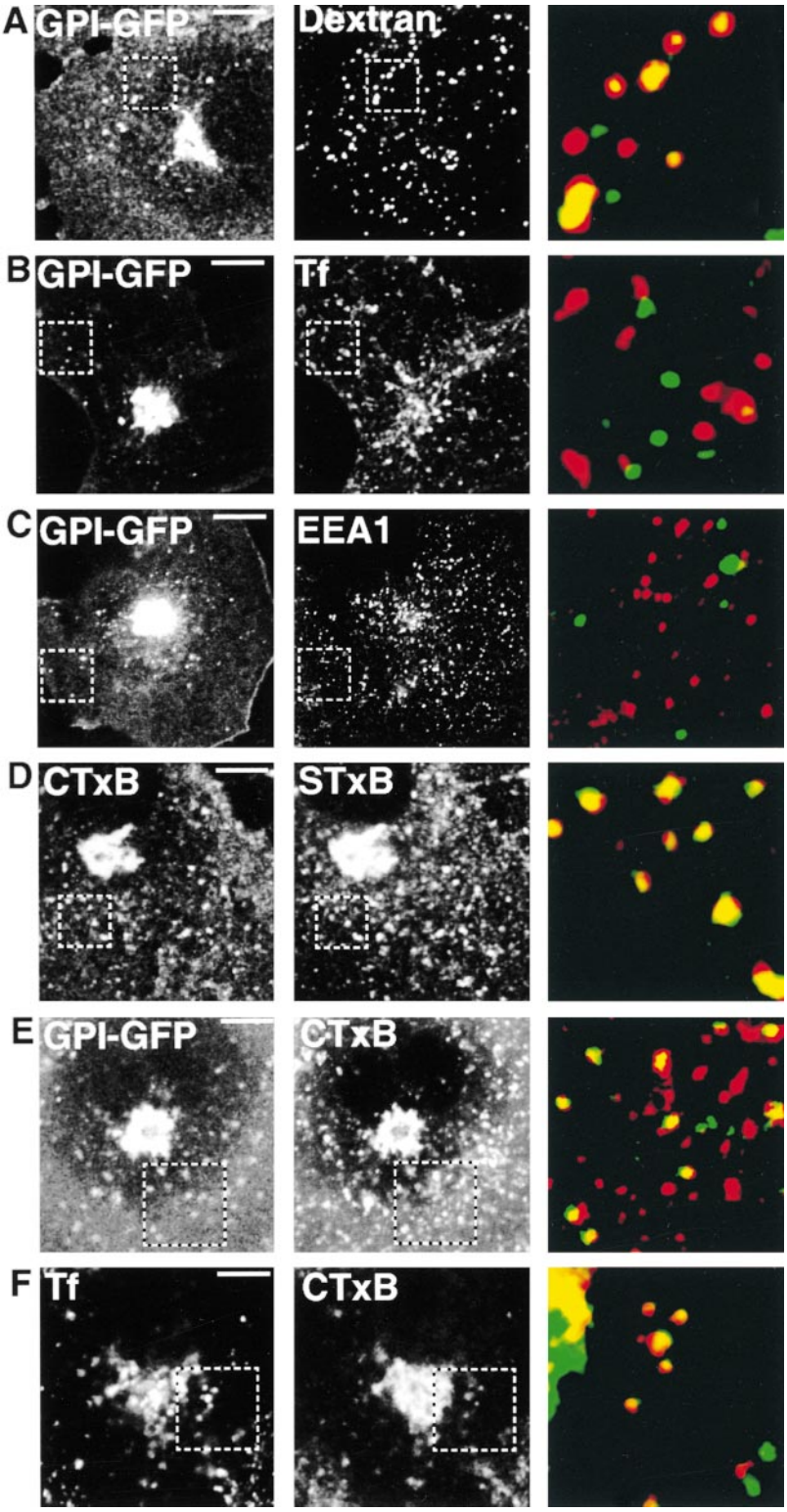

Figure 4. Characterization of endosomes containing GPI-GFP, STxB, and CTxB. In all images the dashed boxes indicate the area shown in the adjacent color panel. Color images have all been processed by adjusting the black level and maximal pixel intensity level in order to aid comparison of the distribution of scattered punctate structures. Cells are COS-7 and were all fixed. (A) Endocytosed 10K Fluoro-Ruby™ dextran labels structures containing GPI-GFP. (B) Endocytosed Cy3-transferrin labels different structures from those containing GPI-GFP. (C) GPI-GFP is not present in EEA1-positive endosomes (D) Endocytosed STxB-Cy3 and CTxB-Cy5 have the same intracellular distribution. (E) Endocytosed CTxB labels structures containing GPI-GFP. (F) Endocytosed CTxB-Cy3 is found both in the Golgi complex, as labeled by GPI-GFP, and in recycling endosomes as labeled by transferrin-Cy5. Bars, 5 μm.

As a more direct test of whether GPI-GFP is taken up via clathrin-coated pits, we used immunoelectron microscopy to ascertain the distribution of GPI-GFP on the cell surface (Fig. 6 F). GPI-GFP was clearly excluded from coated pits and vesicles (linear density of gold particles on the PM was 4.07 ± 0.28 μ^{-1}, in clathrin-coated pits and vesicles it was 0.07 ± 0.02 μ^{-1},and background [mitochondrial] signal was 0.05 ± 0.02 μ^{-1}).

GPI-GFP, STxB, and CTxB Do Not Require Rab5 Activity for Delivery to the Golgi Complex

Early endosome function requires the GTPase rab5, and expression of the GDP-bound form of rab5 (S34N mutant) perturbs early endosomes and inhibits transferrin uptake (Stenmark et al., 1994). In cells expressing rab5 S34N, transferrin uptake was significantly reduced, whereas de-

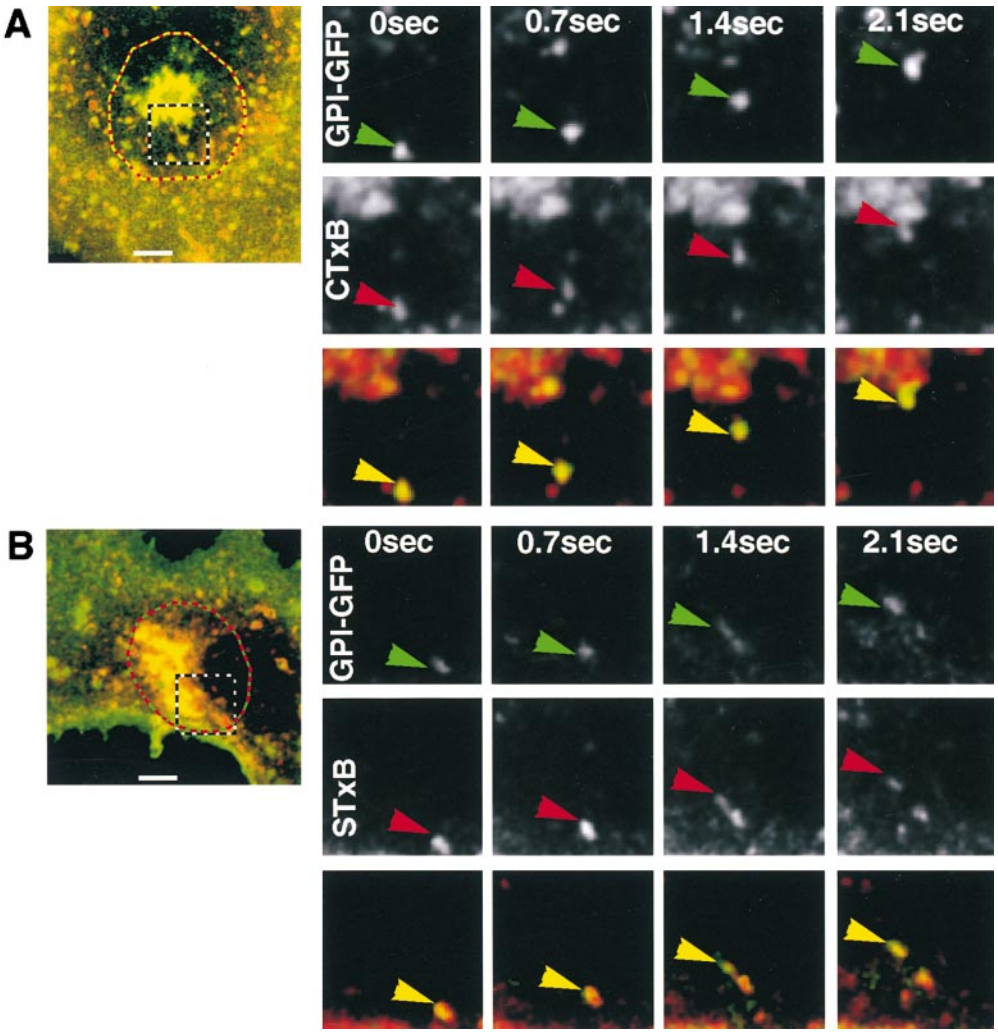

Figure 5. GPI-GFP enters the Golgi complex in endocytic transport intermediates containing both CTxB-Cy3 (A) and STxB-Cy3 (B). The area inside the red and yellow dashed line was photobleached, and the time-lapse images shown are of the boxed region. Times shown are relative to the first image in the series. Supplemental video available at http://www.jcb.org/cgi/content/full/153/3/529/DC1. Bars, 5 μm.

livery of CTxB and STxB (not shown) to the Golgi complex was not significantly affected (Fig. 7 A). Moreover, selective photobleaching of the Golgi pool of GPI-GFP in cells expressing rab5 S34N did not reveal any change in the kinetics of exchange of GPI-GFP between PM and Golgi pools (Fig. 7 B). Thus, the activity of rab5 is not required for delivery of raft markers from the PM to the Golgi complex.

The GTP-bound form of rab5 (Q79L mutant) causes pronounced changes in the morphology of rab5-positive endosomes, without blocking transport of transferrin through these structures (Stenmark et al., 1994). The characteristic morphology of early endosomes under these conditions allowed us to ask whether any GPI-GFP whatsoever is found in such structures. As shown in Fig. 7 C, not even trace amounts of GPI-GFP were found in the enlarged early endosomes produced by rab5 Q79L.

Effect of 20°C Incubation on PM–Golgi Cycling

Incubation at 20°C blocks both uptake of STxB to the Golgi complex and exit from this organelle (Mallard et al., 1998; Van Deurs et al., 1988). We found that uptake of transferrin was not significantly perturbed at this temperature, but both CTxB (Fig. 8 A) and STxB (not shown, but see Mallard et al., 1998) were only taken up into transferrin-containing endosomes, not into the Golgi complex. This led us to test whether the PM–Golgi trafficking of raft markers is differentially sensitive to 20°C treatment. When the Golgi pool of GPI-GFP was photobleached in cells held at 20°C for 40 min, recovery of this pool was effectively blocked (Fig. 8 B), showing that transport of GPI-GFP from the cell surface into the Golgi complex occurs very inefficiently, if at all, under these conditions. Therefore, the PM–Golgi cycling of raft markers appears to be more sensitive to 20°C treatment than the endocytic trafficking of transferrin.

Effect of Cholesterol Depletion on GPI-GFP, STxB, and CTxB Trafficking

Drugs that perturb cholesterol activity are known to inhibit traffic of markers for lipid rafts during both exocytosis and endocytosis, and have been used extensively as tools to differentiate between raft- and nonraft-mediated processes (Keller and Simons, 1998; Orlandi and Fishman, 1998). Filipin, which binds to cholesterol in membranes, had little or no effect on the uptake of either CTxB or STxB to the Golgi complex at a concentration of 1 μg/ml (compare Fig. 8 C with 4 F; in all cases intracellular STxB labeling was indistinguishable from that with CTxB). At a higher concentration of filipin, 10 μg/ml, however, inter-

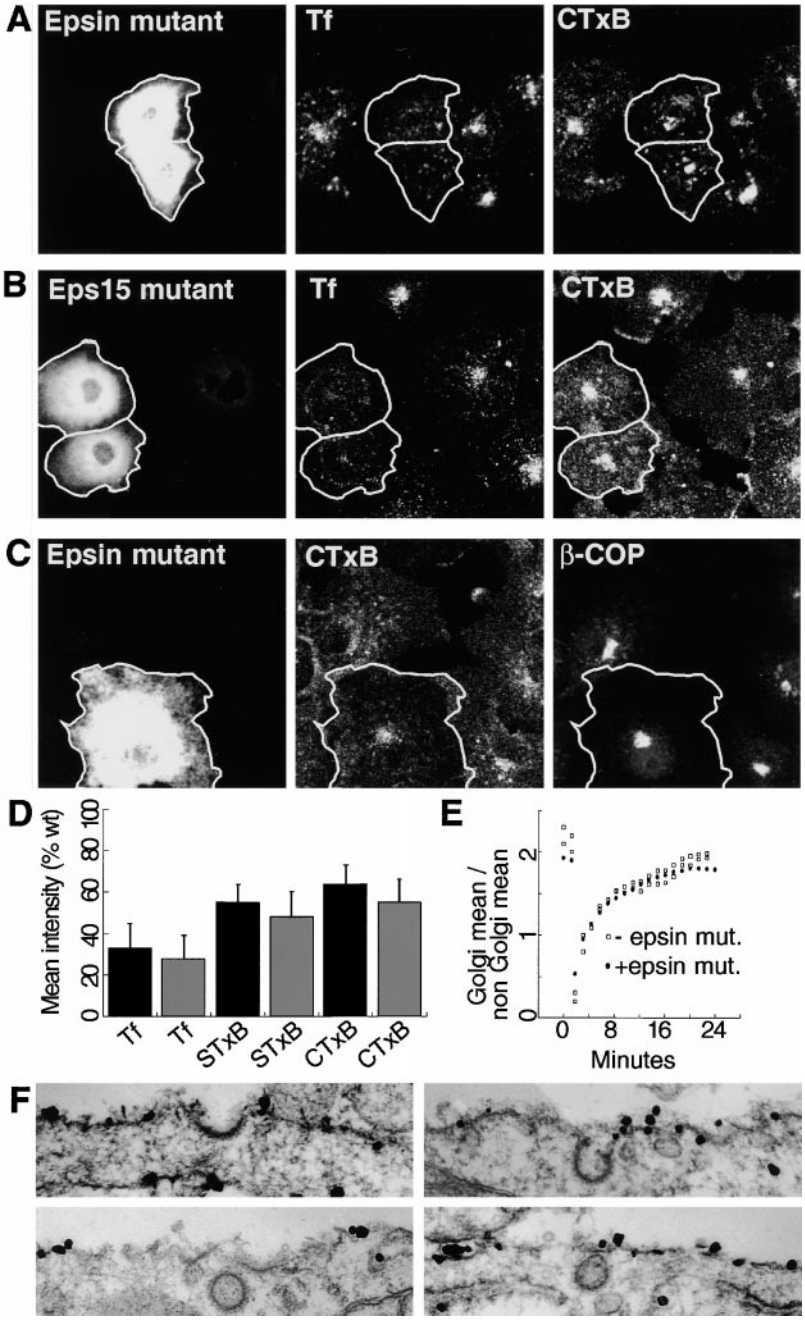

Figure 6. GPI-GFP, STxB, and CTxB are internalized via a clathrin-independent process. (A) Expression of a dominant negative mutant of epsin blocks transferrin-Cy3 uptake more than uptake of CTxB-Cy5. Epsin mutant was expressed by transient transfection of COS-7 cells and detected with anti-FLAG epitope antibodies. Uptake of both markers was for 25 min. (B) Expression of a dominant negative mutant of eps15 blocks transferrin-Cy3 uptake more than uptake of CTxB-Cy5. Eps15 mutant tagged with GFP was expressed by transient transfection of COS-7 cells. Uptake of both markers was for 25 min. (C) Expression of the dominant negative epsin mutant does not block delivery of CTxB-Cy3 to the Golgi complex. The Golgi complex was labeled with antibodies against β-COP and a Cy5-conjugated secondary. (D) Quantitation of the effects of epsin (black bars) and eps15 (grey bars) mutants on transferrin, STxB, and CTxB uptake. Mean fluorescence intensity from STxB, CTxB, or transferrin taken up over 25 min by mutant-transfected cells is expressed as a percentage of the same value from surrounding non-transfected cells. Bars are ± SE; $n \geq 10$. (E) Quantitation of the effects of Epsin mutant on GPI-GFP uptake. The graph shows data from a typical experiment where the Golgi complex in normal (□) or epsin mutant–microinjected (●) cells was photobleached (as in Figs. 2 A and 6 D) at time = 0 s. Mean fluorescence intensity of the Golgi region is expressed as a ratio with the mean fluorescence intensity outside the Golgi as in previous experiments. (F) Immunoelectron microscopy showing distribution of GPI-GFP on the cell surface.

nalization of both CTxB and STxB was reduced and both markers were largely excluded from the Golgi complex. The CTxB and STxB that internalized under these conditions colocalized extensively with transferrin (Fig. 8 C). The amount of transferrin taken up into the cells appeared normal at both filipin concentrations, though treatment with 10 μg/ml filipin caused a slightly increased accumulation in peripheral as opposed to perinuclear endosomes. Thus, cholesterol sequestration by filipin inhibits uptake of STxB and CTxB into the Golgi with little or no effect on their uptake into transferrin-containing endosomes.

To test the effect of cholesterol perturbation on GPI-GFP transport, GPI-GFP–expressing cells were treated with 10 μg/ml filipin for 60 min and examined. GPI-GFP had partially redistributed from the cell surface to the Golgi complex under these conditions (Fig. 8 D). This redistribution most likely occurred as a result of endocytosis, as it occurred similarly in cycloheximide-treated and untreated cells, and as total GFP fluorescence in filipin-treated cells did not increase (total fluorescence was 80 ± 7%, $n = 14$, of starting fluorescence after 1 h in 10 μg/ml filipin). After 60 min at the lower concentration of filipin (1 μg/ml), accumulation of GPI-GFP in the Golgi complex was also apparent (Fig. 8 D). This contrasts with the lack of an effect on CTxB or STxB at this filipin concentration (Fig. 8 C), implying that exit of GPI-GFP from the Golgi complex is more sensitive to filipin treatment than uptake of STxB and CTxB (and potentially GPI-GFP) from the cell surface. These findings show that the trafficking of GPI-GFP, STxB, and CTxB is more sensi-

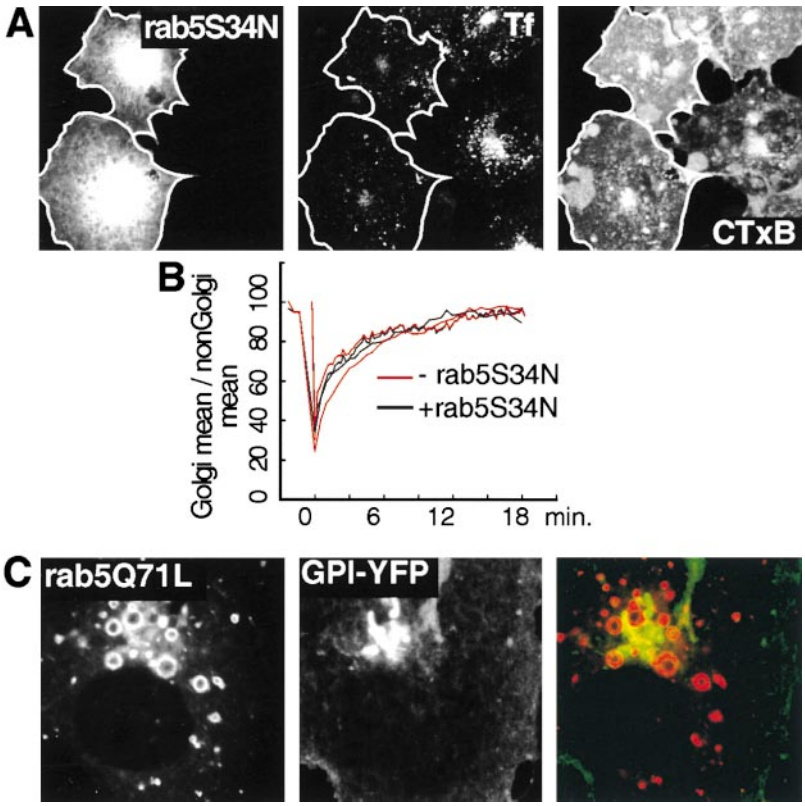

Figure 7. GPI-GFP, CTxB, and STxB do not required rab5 activity for delivery to the Golgi complex. (A) Expression of a dominant negative mutant of rab5 (S34N) blocks intracellular accumulation of transferrin-Cy3 without preventing delivery of CTxB-Cy5 to the Golgi complex. Rab5 mutant tagged with CFP was expressed by transient transfection of COS-7 cells; uptake of both ligands was for 25 min. (B) Kinetics for exchange of GPI-YFP between cell surface and Golgi pools is unaffected by rab5 S34N. Cycloheximide-treated COS-7 cells coexpressing rab5 S34N–CFP and GPI-YFP were loaded with Cy5–transferrin to identify cells where rab5 S34N expression was sufficient to significantly impair transferrin uptake. The Golgi pool of GPI-YFP in these cells was bleached and recovery followed with time as in Fig. 2 A. (C) GPI-YFP does not accumulate in the aberrant early endosomes induced by expression of rab5 Q79L. Rab5 Q79L–CFP and GPI-YFP were coexpressed in COS-7 cells.

tive to cholesterol depletion than the trafficking of transferrin.

Discussion

We have used a minimal GPI-linked protein, GPI-GFP, which associates with detergent-resistant domains on the PM, as a marker to study raft trafficking within cells. Both selective photobleaching and antibody uptake experiments showed that after biosynthetic delivery to the PM, GPI-GFP undergoes continuous internalization and transport to the Golgi complex, followed by recycling back to the PM. The two major steady-state pools of GPI-GFP within the cell, in the Golgi and on the PM, are thus constantly exchanging. This finding led us to investigate more closely the transport route between PM and Golgi that is followed by GPI-GFP in order to understand its relationship to other endocytic routes, and its potential role in raft distribution and function within cells.

One striking feature of the PM–Golgi trafficking pathway followed by GPI-GFP is its kinetic properties. Recovery of GPI-GFP fluorescence in the Golgi after selective photobleaching of this organelle occurred with a half-time of 8 min, indicating a rapid transit time for GPI-GFP molecules moving from PM to the Golgi complex. Kinetic modeling of these data provided rate constants describing exchange of GPI-GFP between PM and Golgi, and implies that on average GPI-GFP molecules reside in the Golgi for only 9 min before being efficiently sorted for return to the PM.

The rapid kinetics of GPI-GFP cycling pointed to the existence of abundant transport intermediates carrying GPI-GFP both into and out from the Golgi. Selective photobleaching to remove PM or Golgi fluorescence allowed us to directly visualize distinct endocytic and exocytic membrane-bound carriers for GPI-GFP. The exocytic carriers required microtubules for movement away from the Golgi apparatus and appeared to fuse directly with the PM (our unpublished observations). Intermediates carrying GPI-GFP into the Golgi region are endocytic in origin, as they contained further markers for lipid rafts, STxB and CTxB, taken up from the cell surface. However, we were unable to track these intermediates from their point of origin and so could not directly identify the organelle where they originate.

To better characterize the endocytic itinerary of GPI-GFP, we compared its distribution with that of a variety of endocytic markers. GPI-GFP was detected in endocytic structures readily accessible to CTxB, STxB, or 10K dextran (fluid phase marker) added at the cell surface. However, we did not detect significant overlap between GPI-GFP and transferrin-containing endosomes. This finding lead us to look more carefully at the requirements for transport of GPI-GFP and other raft markers from the PM to the Golgi complex.

Requirements for Transport of Raft Markers from the PM to the Golgi Complex

CTxB is thought to follow a clathrin-independent pathway from the PM to the Golgi complex (Orlandi and Fishman, 1998). We asked whether internalization of GPI-GFP requires the activity of clathrin-coated pits by overexpressing mutants of either eps15 or epsin, which both disrupt clathrin-mediated endocytosis (Chen et al., 1998; Benmerah et al., 1999). Expression of either mutant protein caused a significant decrease in the amount of transferrin

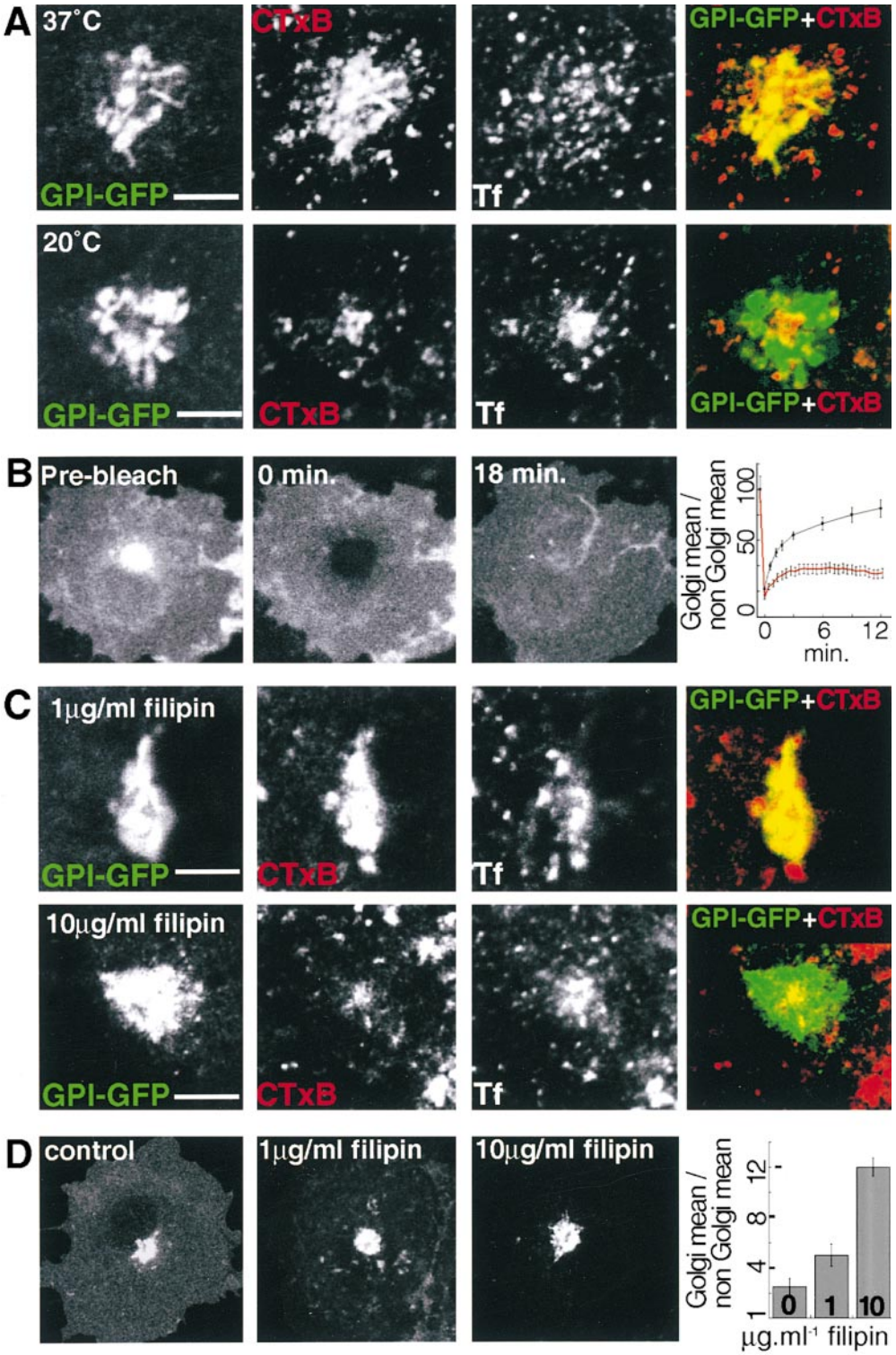

Figure 8. Effect of a 20°C block and cholesterol depletion on GPI-GFP, STxB, and CTxB trafficking. (A) Incubation at 20°C blocks delivery of CTxB-Cy5 to the Golgi complex, but not uptake of transferrin-Cy3. GPI-GFP–expressing COS-7 cells were incubated at the temperature indicated for 40 min before labeling with transferrin-Cy3 and CTxB-Cy5. Color images display the distributions of CTxB (red) and GPI-GFP (green). (B) Incubation at 20°C blocks delivery of GPI-GFP to the Golgi complex. GPI-GFP–expressing COS-7 cells were incubated at the temperature indicated for 40 min before photobleach of the Golgi pool. An equivalent experiment carried out at 37°C is shown in Fig. 2 C. The graph compares the recovery of the Golgi pool of GPI-GFP after photobleaching at 37°C (black line) and 25°C (red lines). The apparent rapid increase in the Golgi pool immediately after photobleaching at 20°C is due to lateral diffusion of GPI-GFP on the PM into the Golgi region. $n = 4$ for both data sets. (C) Filipin treatment blocks delivery of CTxB-Cy5 to the Golgi complex. COS-7 cells were exposed to filipin at the concentrations shown for 1 h. Only the juxtanuclear, Golgi region of the cells is shown. Color images display the distributions of CTxB (red) and GPI-GFP (green). Transferrin-Cy3 and CTxB-Cy5 uptake were as described in Materials and Methods. (D) Filipin treatment causes redistribution of GPI-GFP from the cell surface to the Golgi complex. Fluorescence images are of GPI-GFP expressed in COS-7 cells 1 h after treatment with the concentration of filipin shown. Note that to avoid pixel saturation, different imaging conditions are used for each image. The bar graph shows quantitation of the mean fluorescence intensity within the Golgi region as a ratio with that of the non-Golgi region. $n \geq 10 \pm$ SE. Total GPI-GFP fluorescence intensity in filipin-treated cells changed slightly; total fluorescence was 80 ± 7%, $n = 14$, of initial fluorescence after 1 h in 10 μg/ml filipin. Bars, 5 μm.

taken up into cells, but did not perturb cycling of GPI-GFP between PM and Golgi pools. Furthermore, immunogold labeling revealed that GPI-GFP on the cell surface is largely excluded from clathrin-coated pits. In cells expressing eps15 or epsin mutants, delivery of STxB and CTxB to the Golgi complex was unaffected, despite the fact that total uptake of the toxins from the cell surface decreased. These results support a mechanism for uptake

of GPI-GFP, as well as of a proportion of the total STxB and CTxB internalized under normal conditions, that does not involve clathrin-coated pits and indicates that uptake via this mechanism leads to delivery to the Golgi complex.

Further results suggest that, after internalization, raft markers continue to utilize endocytic machinery distinct from that used by transferrin. In cells expressing rab5 S34N, which interferes with early endosome function and hence uptake of transferrin (Stenmark et al., 1996), delivery of STxB and CTxB to the Golgi were unaffected, and selective photobleaching revealed the kinetics of GPI-GFP trafficking to be unaltered. Furthermore, overexpression of rab5 Q79L caused accumulation of aberrant early endosomal membranes with a characteristic and readily identified morphology, and these membranes were devoid of GPI-GFP.

The function and organization of rafts is perturbed by depletion of cholesterol from membranes, providing a tool to discriminate between raft- and nonraft-dependent processes (Simons and Ikonen, 1997; Keller and Simons, 1998). Sequestration of cholesterol by filipin had a significant effect on the trafficking of GPI-GFP, CTxB, and STxB. Filipin treatment of cells at concentrations that did not significantly affect transferrin uptake blocked delivery of CTxB and STxB to the Golgi complex (Orlandi and Fishman, 1998). It also resulted in the accumulation of GPI-GFP in the Golgi complex and a corresponding depletion from the cell surface, implying that the point in the cycling itinerary of GPI-GFP which is most acutely sensitive to cholesterol levels is Golgi exit.

The PM–Golgi cycling of raft markers was also differentially sensitive to 20°C treatment compared with other endocytic pathways. Indeed, incubation of cells at 20°C resulted in effects that were similar to those of cholesterol depletion. The reduced ability of raft markers (and presumably raft lipids) to recycle to the Golgi at 20°C could well be related to the more general block in membrane trafficking through the secretory pathway observed under these conditions.

Previous work has suggested that many proteins which traffic from PM to the Golgi complex, including TGN38, furin, and STxB, are taken up via clathrin-coated pits into transferrin-positive recycling endosomes before being sorted out for subsequent delivery to the Golgi complex (Ghosh et al., 1998; Mallard et al., 1998). Our findings raise the possibility that the itinerary of raft markers en route to the Golgi is distinct from the pathway followed by transferrin. However, we can not directly exclude the possibility that GPI-GFP does, at some stage, pass through the same endosomes as transferrin, in which case the observed differences in steady-state distribution would be explained by rapid sorting of GPI-GFP out of the transferrin-positive compartment. Despite this caveat, previous work on toxin uptake clearly shows that internalization via clathrin-coated pits is not functionally equivalent to internalization via a separate, cholesterol-requiring mechanism, so it seems unlikely that these distinct uptake pathways lead to delivery to a common endocytic organelle (Orlandi and Fishman, 1998; Schapiro et al., 1998).

Different Endocytic Distributions for Different Raft Markers

We asked whether endogenous GPI-anchored proteins behave in the same way as GPI-GFP. The distribution of endogenous CD59 and the behavior of a GFP fusion based on this GPI-anchored protein in selective photobleaching experiments, were identical to that of GPI-GFP, indicating that trafficking of these molecules between the cell surface and the Golgi complex reflects a more general constitutive pathway, rather than one unique to GPI-GFP. A similar pathway may be followed by a GPI-anchored heparan sulfate proteoglycan, as previous work shows that after this proteoglycan has been biotinylated at the cell surface it can subsequently undergo addition of heparan sulfate side chains in the Golgi complex (Fransson et al., 1995). Given our findings, it is likely that raft lipids continuously circulate between PM and Golgi pools. Consistent with this, studies on the uptake of exogenous raft lipids have shown that these molecules traffic from the PM to the Golgi complex, as evidenced by Golgi-specific modifications acquired by these lipids after uptake from the cell surface (Giglioni et al., 1990; Martin and Pagano, 1994; Schwarzmann et al., 1995).

The PM–Golgi pathway described by GPI-GFP appears to be raft specific, yet not all raft-associated molecules follow it. For the folate receptor (which is GPI-anchored), our data confirmed a distribution within transferrin-labeled early and recycling endosomes that has previously been described in detail by Mayor et al. (1998). Moreover, whilst a proportion of the total internalized STxB and CTxB is delivered to the Golgi apparatus in the same manner as GPI-GFP, the remainder is internalized in a clathrin-dependent fashion. Both CTxB and STxB accumulate in transferrin-labeled compartments as well as the Golgi complex. Folate receptor enters transferrin-labeled endosomes significantly more efficiently (2% per min; Mayor et al., 1998) than the minimal GPI-anchored protein, GPI-GFP moves to the Golgi complex (0.5% per min determined from our photobleaching experiments). Accumulation of raft-associated proteins, such as the folate receptor within transferrin-containing endosomes, could thus be mediated by additional sorting signals.

Further Questions

The precise sequence of trafficking events required to get GPI-GFP and other raft markers from the PM to the Golgi complex is currently not clear. The presence of GPI-GFP in endocytic structures which are readily accessible to fluid-phase (10K dextran) uptake implies that if GPI-GFP passes through these structures en route to the Golgi, further sorting step or steps must occur so as to exclude lumenal volume relative to membrane surface area, as the Golgi complex itself it not readily labeled by fluid-phase uptake. Similarly, the structures responsible for budding of GPI-GFP from the PM remain to be ascertained.

Given that there is likely to be a considerable flux of lipid rafts between the PM and the Golgi complex, what might be the cell biological significance of this pathway? Lipid rafts have been shown to play a role in sorting at the TGN of both polarized and nonpolarized cells, and the components of these rafts may well play a more general role in Golgi organization (Bretscher and Munro, 1993; Si-

mons and Ikonen, 1997). It has been presumed that the lipid and protein components of these membrane domains are supplied in the Golgi complex by new synthesis, but our results raise the possibility that recycling of rafts from the PM to the Golgi also plays an important role in this process. A related potential function of raft recycling is in the selective endocytosis of particular cell surface components during generation of polarized cell surface domains. A further potential role is in regulation of cell-signaling events (Stauffer and Meyer, 1997; Brown and London, 1998). Many cell surface receptors and signaling molecules are recruited into detergent-resistant domains, so the internalization of these domains may well play an important role in signaling events. The existence of a specific marker for this membrane cycling pathway, GPI-GFP, will allow these and other questions related to the functional significance of the pathway to be addressed in future studies.

We thank all those who contributed antibodies and reagents. We especially thank L. Johannes for generously providing the STxB.

B.J. Nichols was funded by an International Prize Travelling Research Fellowship from the Wellcome Trust (London, UK). A.K. Kenworthy was funded by a fellowship from the National Research Council. R. Lodge was funded by a Canadian MRC postdoctoral fellowship.

Submitted: 30 October 2000
Revised: 7 March 2001
Accepted: 7 March 2001

References

Benting, J.H., A.G. Rietveld, and K. Simons. 1999. N-glycans mediate the apical sorting of a GPI-anchored, raft-associated protein in Madin-Darby canine kidney cells. *J. Cell Biol.* 146:313–320.

Benmerah, A., M. Bayrou, N. Cerf-Bensussan, and A. Dautry-Varsat. 1999. Inhibition of clathrin-coated pit assembly by an Eps15 mutant. *J. Cell Sci.* 112: 1303–1311.

Bretscher, M.S., and S. Munro. 1993. Cholesterol and the Golgi apparatus. *Science*. 261:1280–1281.

Brown, D.A., and E. London. 1998. Functions of lipid rafts in biological membranes. *Annu. Rev. Cell Dev. Biol.* 14:111–136.

Chen, H., S. Fre, V.I. Slepnev, M.R. Capua, K. Takei, M.H. Butler, P.P. Di Fiore, and P. De Camilli. 1998. Epsin is an EH-domain-binding protein implicated in clathrin-mediated endocytosis. *Nature*. 394:793–797.

Davies, A., and P.J. Lachmann. 1993. Membrane defence against complement lysis: the structure and biological properties of CD59. *Immunol. Res.* 12:258–275.

Fransson, L.A., G. Edgren, B. Havsmark, and A. Schmidtchen. 1995. Recycling of a glycosylphosphatidylinositol-anchored heparan sulphate proteoglycan in skin fibroblasts. *Glycobiology*. 5:407–415.

Ghosh, R.N., W.G. Mallet, T.T. Soe, T.E. McGraw, and F.R. Maxfield. 1998. An endocytosed TGN38 chimeric protein is delivered to the TGN after trafficking through the endocytic recycling compartment in CHO cells. *J. Cell Biol.* 142:923–936.

Giglioni, A., M. Pitto, V. Chigorno, L. Zorzino, and R. Ghidoni. 1990. Subcellular metabolism of exogenous GM1 ganglioside in normal human fibroblasts. *Biochem. Int.* 22:85–94.

Hirschberg, K., C.M. Miller, J. Ellenberg, J.F. Presley, E.D. Siggia, R.D. Phair, and J. Lippincott-Schwartz. 1998. Kinetic analysis of secretory protein traffic and characterization of Golgi to plasma membrane transport intermediates in living cells. *J. Cell Biol.* 143:1485–1503.

Jacquez, J.A. 1996. Compartmental Analysis in Biology and Medicine. 3rd edition. Biomedware, Ann Arbor, MI. 512 pp.

Katagiri, Y.U., T. Mori, H. Nakajima, C. Katagiri, T. Taguchi, T. Takeda, N. Kiyokawa, and J. Fujimoto. 1999. Activation of Src family kinase Yes induced by Shiga toxin binding to globotriaosyl ceramide Gb3/CD77 in low density, detergent-insoluble microdomains. *J. Biol. Chem.* 274:35278–35282.

Keller, P., and K. Simons. 1998. Cholesterol is required for surface transport of influenza virus hemagglutinin. *J. Cell Biol.* 140:1357–1367.

Kenworthy, A.K., and M. Edidin. 1998. Distribution of a glycosylphosphatidylinositol-anchored protein at the apical surface of MDCK cells examined at a resolution of <100 Å using imaging fluorescence resonance energy transfer. *J. Cell Biol.* 142:68–84.

Lisanti, M.P., I.W. Caras, T. Gilbert, D. Hanzel, and E. Rodriguez-Boulan. 1990. Vectorial apical delivery and slow endocytosis of a glycolipid-anchored fusion protein in transfected MDCK cells. *Proc. Natl. Acad. Sci. USA*. 87: 7419–7423.

Mallard, F., A. Claude, D. Tenza, J. Salamero, B. Goud, and L. Johannes. 1998. Direct pathway from early/recycling endosomes and the Golgi apparatus revealed through the study of Shiga toxin B subunit. *J. Cell Biol.* 143:973–990.

Martin, O.C., and R.E. Pagano. 1994. Internalization and sorting of a fluorescent analogue of glucosylceramide to the Golgi apparatus of human skin fibroblasts: utilization of endocytic and nonendocytic transport mechanisms. *J. Cell Biol.* 125:769–781.

Mayor, S., and F.R. Maxfield. 1995. Insolubility and redistribution of GPI-anchored proteins at the cell surface after detergent treatment. *Mol. Biol. Cell.* 6:929–944.

Mayor, S., S. Sabharanjak, and F.R. Maxfield. 1998. Cholesterol-dependent retention of GPI-anchored proteins in endosomes. *EMBO (Eur. Mol. Biol. Organ.) J.* 17:4626–4638.

Nehls, S., E.L. Snapp, N.B. Cole, K.J.M. Zaal, A.K. Kenworthy, T.H. Roberts, J. Ellenberg, J.F. Presley, E. Siggia, and J. Lippincott-Schwartz. 2000. Dynamics and retention of misfolded proteins in native ER membranes. *Nat. Cell Biol.* 2:288–295.

Orlandi, P.A., and P.H. Fishman. 1998. Filipin-dependent inhibition of cholera toxin: evidence for toxin internalization and activation through caveolae-like domains. *J. Cell Biol.* 141:905–915.

Parton, R.G., B. Joggerst, and K. Simons. 1994. Regulated internalization of caveolae. *J. Cell Biol.* 127:1199–1215.

Polishchuk, R.S., E.V. Polishchuk, P. Marra, S. Alberti, R. Buccione, A. Luini, and A.A. Mironov. 2000. Correlative light-electron microscopy reveals the tubular-saccular ultrastructure of carriers operating between Golgi apparatus and plasma membrane. *J. Cell Biol.* 148:45–58.

Pralle, A., P. Keller, E. Florin, K. Simons, and J.K. Horber. 2000. Sphingolipid-cholesterol rafts diffuse as small entities in the plasma membrane of mammalian cells. *J. Cell Biol.* 148:997–1008.

Presley, J.F., S. Mayor, T.E. McGraw, K.W. Dunn, and F.R. Maxfield. 1997. Bafilomycin A1 treatment retards transferrin receptor recycling more than bulk membrane recycling. *J. Biol. Chem.* 272:13929–13936.

Rothberg, K.G., Y.-S. Ying, J.F. Kolhouse, B.A. Kamen, and R.G.W. Anderson. 1990. The glycophospholipid-linked folate receptor internalizes folate without entering the clathrin-coated pit endocytic pathway. *J. Cell Biol.* 110: 637–649.

Sandvig, K., S. Olsnes, J.E. Brown, O.W. Petersen, and B. van Deurs. 1989. Endocytosis from coated pits of Shiga toxin: a glycolipid-binding protein from *Shigella dysenteriae* 1. *J. Cell Biol.* 108:1331–1343.

Schapiro, F.B., C. Lingwood, W. Furuya, and S. Grinstein. 1998. pH-independent retrograde targeting of glycolipids to the Golgi complex. *Am. J. Physiol.* 274:319–332.

Schwarzmann, G., P. Hofmann, U. Putz, and B. Albrecht. 1995. Demonstration of direct glycosylation of nondegradable glucosylceramide analogs in cultured cells. *J. Biol. Chem.* 270:21271–21276.

Simons, K., and E. Ikonen. 1997. Functional rafts in cell membranes. *Nature*. 387:569–572.

Skretting, G., M.L. Torgersen, B. Van Deurs, and K. Sandvig. 1999. Endocytic mechanisms responsible for uptake of GPI-anchored diptheria toxin receptor. *J. Cell Sci.* 112:3899–3909.

Smart, E.J., C. Mineo, and R.G. Anderson. 1996. Clustered folate receptors deliver 5-methyltetrahydrofolate to cytoplasm of MA104 cells. *J. Cell Biol.* 134: 1169–1177.

Stauffer, T.P., and T. Meyer. 1997. Compartmentalized IgE receptor-mediated signal transduction in living cells. *J. Cell Biol.* 139:1447–1454.

Stenmark, H., R. Aasland, B.H. Toh, and A. D'Arrigo. 1996. Endosomal localization of the autoantigen EEA1 is mediated by a zinc-binding FYVE finger. *J. Biol. Chem.* 271:24048–24054.

Stenmark, H., R.G. Parton, O. Steele-Mortime, A. Lutcke, J. Gruenberg, and M. Zerial. 1994. Inhibition of rab5 GTPase activity stimulates membrane fusion in endocytosis. *EMBO (Eur. Mol. Biol. Organ.) J.* 13:1287–1296.

Van Deurs, B., K. Sandvig, O.W. Petersen, S. Olsnes, K. Simons, and G. Griffiths. 1988. Estimation of the amount of internalized ricin that reaches the trans-Golgi network. *J. Cell Biol.* 106:253–267.

Varma, R., and S. Mayor. 1998. GPI-anchored proteins are organized in submicron domains at the cell surface. *Nature*. 394:798–801.

Zaal, K.J., C.L. Smith, R.S. Polishchuk, N. Altan, N.B. Cole, J. Ellenberg, K. Hirschberg, J.F. Presley, T.H. Roberts, E. Siggia, R.D. Phair, and J. Lippincott-Schwartz. 1999. Golgi membranes are absorbed into and reemerge from the ER during mitosis. *Cell*. 99:589–601.

Zurzolo, C., M.P. Lisanti, I.W. Caras, L. Nitsch, and E. Rodriguez-Boulan. 1993. Glycosylphosphatidylinositol-anchored proteins are preferentially targeted to the basolateral surface in Fischer rat thyroid epithelial cells. *J. Cell Biol.* 121:1031–1039.